Proceedings of the PVP2011
Pressure Vessels and Piping Division Conference
17-21 July 2011, Baltimore, Maryland, USA

PVP2011-57307

PROGRESS TOWARDS THE REVISION OF BS 7910

Isabel Hadley
TWI Ltd
Granta Park
Great Abington
Cambridge
CB21 6AL
UK

ABSTRACT

BS 7910, the UK procedure for the assessment of flaws in metallic structures, is being revised with a view to publication in 2012. Like the existing procedure, the new procedure will address all major failure/damage mechanisms, namely fracture, fatigue, creep and corrosion, and is intended to be used across a range of industry sectors and component types. There are several major proposed changes, which draw mainly on the existing BS 7910 procedures, the UK nuclear industry's R6 document and the European FITNET procedure. The most far-reaching changes are in Section 7 (fracture) and related annexes. Here, the modifications include:

- a re-structuring of the fracture assessment procedures from their present form (Levels 1-3) to a new hierarchy based on Options 1-3, which are more compatible with the current R6 and FITNET approaches
- revised treatment of flaw interaction,
- a new annex (Annex N) permitting analysis under conditions of reduced crack tip constraint,
- a new annex (I) addressing analysis of weld strength mismatch,
- a revised residual stress compendium (Annex Q).

As part of the revision, all annexes will be reviewed and edited where necessary, and a new annex on non-destructive examination (NDE) will be included for the first time.

In view of the fact that many of the major changes concern the fracture assessment clauses, this paper presents a case study based on the analysis of a fully-circumferential flaw in a pipeline girth weld. The basic assessment Options (1 and 2) given in the new procedure are used to analyse the flaw, and three more advanced techniques (constraint-based assessment, assessment using an idealised residual stress distribution and analysis based on weld strength mismatch) are also applied.

INTRODUCTION

The history and future of the BS 7910 flaw assessment procedure [1] and its relationship to other European fitness for service (FFS) procedures such as the UK nuclear industry procedure R6 [2] and FITNET [3] were described in earlier ASME PVP conference papers [4][5]. Considerable progress has been made in the past year on the drafting of all parts of the procedure, which is due for publication around 2012. Several of the papers presented at the current PVP conference will cover particular aspects of the new procedure, eg flaw interaction, residual stress, plastic collapse and creep analysis. Because of the fact that the main changes to the procedure will be in the area of fracture assessment, this paper presents a case study, based on the new fracture assessment clauses and annexes, illustrating various features of the new procedure.

NOMENCLATURE

A_2:	a measure of crack tip constraint
a/W:	relative crack length in test specimen
CCT;	centre-cracked tension specimen
CTOD:	Crack Tip Opening Displacement (a measure of fracture toughness)
E:	Young's modulus
ECA:	Engineering Critical Assessment
FAD:	Failure Assessment Diagram
FAL:	Failure Assessment Line
F_e^B:	limit load for base material
F_e^M:	limit load for mismatched weld
FFS:	Fitness for Service
$J_{0.2}$:	value of J-integral at initiation of ductile tearing (a measure of fracture toughness)
K_J:	fracture toughness in terms of K, derived from the J-integral (a of measure fracture toughness)
K_{mat},	characteristic fracture toughness

K_r: Proximity to failure by brittle or ductile fracture
L_r: Proximity to failure by plastic collapse
M: mismatch (ratio of weld metal to parent metal yield strength)
N: strain hardening exponent
N_M: strain hardening exponent for a mismatched weld
P_m: applied primary membrane stress
Q: a measure of crack tip constraint
Q_m: membrane component of residual stress
RS: residual stress
SENB: single edge-notched bend specimen
SENT: single edge-notched tension specimen
T: a measure of crack tip constraint
β_T: a measure of crack tip constraint, derived from T:
ε_{ref}: reference strain
σ_f: flow strength (mean of σ_Y and σ_{UTS})
σ_{UTS}: ultimate tensile strength
σ_Y: yield or 0.2% proof strength

CASE STUDY

The case study used to illustrate the main changes to BS 7910 concerns the analysis of a fully circumferential internal flaw at the root of a pipeline girth weld, as shown in Figure 1 and Figure 2. The linepipe material, the pipeline geometry and the welding process and procedure used for the girth weld are fairly typical of offshore pipelines; small-scale testing of the weldment was carried out as part of an experimental/analytical study by Zhou [6][7]. Further details of the materials, and of the geometry and loading considered in the case study are shown in Table 1. The pipe is assumed to be subjected to an axial stress, P_m, of 50% of the actual yield strength of the parent pipe (this fairly low value of P_m was chosen to avoid the potentially confusing effects of allowing residual stress relaxation to occur as primary stress is increased, as envisaged by both the current and future editions of BS7910). The scenario is then analysed using a variety of different procedures, taken from the current draft of the new BS 7910:

- Basic assessment using Options 1 and 2, ie treating the pipe as a homogeneous material, the fracture toughness of which is determined from standard fracture mechanics tests on the weld metal, but whose tensile properties are assumed to be those of the parent (weaker) material.
- Constraint-based assessment using Annex N of the new BS 7910. This allows the user to determine an 'equivalent' fracture toughness for the structure of interest, based on low-constraint fracture toughness testing and using constraint parameters to match the levels of crack tip constraint in the structure with those of appropriate test specimens.
- Analysis taking into account the residual stress (RS) distribution library of Annex Q. Whilst much of the material in this annex is not new, the revised presentation and improved user-friendliness of the material is likely to promote wider use of the annex.
- Analysis taking account of the strength mismatch, M, between weld metal and parent metal. This uses information in the new Annex I and Annex P.

Basic assessment (Options 1 and 2)

The flaw in a girth weld, described in Figure 1 - Figure 3 and Table 1, was first analysed as a known flaw based on the following assumptions:

- Tensile properties: equal to those of the parent material (the weaker component in the weldment), even though the flaw is in the weld metal. This is in line with the current advice in BS 7910.
- Fracture toughness: the initiation toughness ($J_{0.2mm}$) of the weld metal, as determined from tearing resistance curves (R-curves) using deeply-notched SENB specimens, was used to define the characteristic toughness, K_{mat}.
- Residual stress; the Level 1 assumption was used, ie it was assumed that the welding residual stress transverse to the weld (ie the component acting axially with respect to the pipe) acts across the entire cross-section of the weld as a secondary stress with magnitude Q_m=478N/mm^2, equivalent to the room temperature yield strength of the parent material.

The Failure Assessment Line (FAL) for the Option 1 analysis is given by:

$$K_r = f(L_r) = \left(1+0.5L_r^2\right)^{-0.5}\left\{0.3+0.7\exp\left(-\mu L_r^6\right)\right\} \quad (1)$$

for L_r<1, where:

$$\mu = \min\left[0.001\frac{E}{\sigma_Y};0.6\right] \quad (2)$$

followed by:

$$f(L_r) = f(1)L_r^{(N-1)/2N} \quad (3)$$

for 1< L_r<$L_{r,max}$, where N is an estimate of the strain hardening exponent, given by:

$$N = 0.3\left[1-\left(\frac{\sigma_Y}{\sigma_{UTS}}\right)\right] \quad (4)$$

and

$$L_{r,\max} = \frac{\sigma_f}{\sigma_Y} \quad (5)$$

where σ_f is the flow strength of the material.

For the Option 2 FAD, the assessment line was derived from the full stress-strain curve of the parent metal:

$$K_r = f(L_r) = \left[\frac{E\varepsilon_{ref}}{L_r\sigma_Y} + \frac{{L_r}^3\sigma_Y}{2E\varepsilon_{ref}} \right]^{-0.5} \quad (6)$$

where ε_{ref} is the true strain obtained from the uniaxial tensile stress-strain curve at a true stress $L_r\sigma_Y$ (this is identical to the current BS 7910 Level 2b/Level 3b FAD).

Results of the assessment using Options 1 and 2 are shown in Figure 4. The Option 1 Failure FAL is based on the tensile properties (0.2% proof strength and UTS) of the parent material, which shows continuous yielding, while the Option 2 method uses the whole stress-strain curve for the parent material to generate an alternative FAL with a slighter larger 'safe' area. The Level 2a FAL from the current (2005) edition of BS 7910 is also shown for comparison. The Level 2a and Option 1 FALs are seen to be very similar, but use of the Option 2 FAL produces a larger 'safe' area and thus a higher safety margin, even though the analysis point (L_r=0.562, K_r=0.498) remains the same in all three cases.

Constraint-based assessment (Annex N)

Constraint-based assessment of the weld was made possible by the fact that room temperature tearing resistance curves (R-curves) had been generated for the weld metal, using both standard and low-constraint fracture toughness tests as follows:

- SENB specimens, a/W=0.16, 0.35, 0.51, 0.7; side-grooved 25mm thick x 50mm wide specimens
- SENT specimens, a/W=0.4, plane-sided, surface-notched 50mm thick x 25mm wide (ie 'pipeline' SENT geometry, fixed grip condition)
- CCT specimens, a/W=0.4, plane-sided, 10mm thick x 160mm high

Note that the type of SENT specimen considered in this work is routinely used in the ECA of pipelines, in particular under conditions of high axial strain. It is intended to reproduce the constraint conditions at the crack tip in a uniaxially loaded pipeline (eg during installation), bypassing the need for detailed constraint calculations on a case-by-case basis. Whilst the SENT specimens, which were notched from the surface, sampled a different notch orientation compared with the other specimens, previous work on the same welds had shown R-curves (in terms of CTOD, on plane-sided specimens) for surface-notched and through-thickness notched specimens to be similar. The SENT specimens were therefore considered to differ from SENB and CCT only in terms of constraint conditions.

Zhou [6] [7] also carried out numerical analysis to derive T-stress, Q and A_2 (a constraint parameter not currently considered in the new BS 7910) for all specimens. These are not necessarily needed for the application of constraint-based analysis using the new BS 7910, since Annex N includes tables of constraint parameters for particular specimen geometries, collated from existing literature. Nevertheless, they provide an additional source of information specific to the case studied, and a comparison is provided later between the constraint parameters determined directly by Zhou and those derived from Annex N.

Zhou's numerical analyses were also used to decide on the constraint parameter to be used in the case study, ie T-stress or Q. It was noted that, for the case of the four sets of SENB specimens tested, there was a trend between the initiation toughness $J_{0.2mm}$ and the relative crack depth a/W, which could be expressed either in terms of a relationship between $J_{0.2mm}$ and T-stress (as calculated directly from Zhou's work), or one between $J_{0.2mm}$ and Q. Because the trends were similar (see Figure 5 and Figure 6), a decision was made to use the simpler elastic T-stress method in the first instance, and the data was subsequently analysed using Annex N only, ie as if no FEA had been carried out on the specific specimens tested.

The fracture toughness at initiation of tearing, $J_{0.2mm}$, was reformulated in terms of $K_{J0.2mm}$ using the relationship:

$$K_J = \sqrt{\frac{JE}{(1-\upsilon^2)}} \quad (7)$$

A value β_T was then calculated for each of the SENB specimens from Section N.4.2.2.1.6 of the new BS 7910, ie:

$$\beta_T = X_0 + X_1\left(\frac{a}{W}\right) + X_2\left(\frac{a}{W}\right)^2 + X_3\left(\frac{a}{W}\right)^3 + X_4\left(\frac{a}{W}\right)^4 + X_5\left(\frac{a}{W}\right)^5 + X_6\left(\frac{a}{W}\right)^6 \quad (8)$$

for $0 \le a/W \le 0.8$, where the coefficients X_0 to X_6 are given below for a specimen with width to thickness ratio (W/B) of 2:

X_0	X_1	X_2	X_3	X_4	X_5	X_6
-0.7887	-0.1795	32.904	-153.45	316.11	-308.47	115.18

In contrast with much published work (which shows 'T' normalised by some remote stress), the tables in Annex N show 'T' normalised by reference stress (ie β_T), to allow use in a FAD-based analysis. In this case, the plane strain von Mises limit load from Miller was used to derive β_T.

The results are summarised in Figure 7 as a relationship between β_T and $K_{J0.2mm}$ for SENB specimens only. The reason for considering only SENB specimens at this stage is that testing of SENB specimens (albeit for deeply-notched specimens) is fully standardised, so it was considered that the analysis should be weighted towards these data.

There appears to be a moderate dependence of toughness (in terms of $K_{J0.2mm}$) on constraint (in terms of β_T), which can be expressed by the trendline and associated equation given in Figure 7. Consequently, it should be possible to collapse all the results (SENB, SENT and CCT) onto a single curve if an

appropriate constraint indexing parameter is used. Moreover, this curve could be used to calculate the expected fracture toughness in a geometry not hitherto tested, eg the fully circumferential internal flaw in a cylinder, considered in the case study but not directly tested.

Section N.4.2.2.1.4 is now used to define β_T for the SENT specimen:

X_0	X_1	X_2	X_3	X_4
-0.5889	-0.0128	0.5512	4.651	-4.6703

$$\beta_T = X_0 + X_1\left(\frac{a}{W}\right) + X_2\left(\frac{a}{W}\right)^2 + X_3\left(\frac{a}{W}\right)^3 + X_4\left(\frac{a}{W}\right)^4 \quad (9)$$

for $0 \le a/W \le 0.6$, and specimen length to width ratio of 6, assuming a pin-loaded condition.

For a/W=0.4, β_T=-0.328, so the predicted value of toughness for the SENT specimens (based on the SENB trendline shown in Figure 7) is 240.4MPa√m. The actual value determined in the laboratory was somewhat higher at 252MPa√m, as shown in Figure 8, and possible reasons for the discrepancy are discussed later (see the section 'Comparison of β_T solutions from Annex N with those derived directly from FEA of specimens').

Section N.4.2.2.1.1 can be used to derive β_T for the CCT geometry:

X_0	X_1	X_2	X_3	X_4
-1.1547	1.1511	-0.7826	0.4751	-0.1761

$$\beta_T = X_0 + X_1\left(\frac{a}{W}\right) + X_2\left(\frac{a}{W}\right)^2 + X_3\left(\frac{a}{W}\right)^3 + X_4\left(\frac{a}{W}\right)^4 \quad (10)$$

for $0 \le a/W \le 0.6$ and a specimen height/width ratio of 1.5.

For a/W=0.4, β_T=-0.794, so the predicted toughness of a CCT specimen is 316.7MPa√m, as shown in Figure 8. Paradoxically, Zhou's results show just $K_{J0.2mm}$=202MPa√m for the CCT specimens, lower than the trend curve would suggest. These results need to be considered further, eg there appears from the photos to have been fracture path deviation, which would have invalidated the calculation of fracture toughness. The CCT results are therefore not further considered in this work.

For the case of the 3mm high flaw in a 27.8mm thick pipe, N.4.2.2.2.1 gives:

X_0	X_1	X_2	X_3	X_4	X_5	X_6
-0.51	-0.3175	2.7925	-9.3521	23.048	-26.86	10.808

$$\beta_T = X_0 + X_1\left(\frac{a}{t}\right) + X_2\left(\frac{a}{t}\right)^2 + X_3\left(\frac{a}{t}\right)^3 + X_4\left(\frac{a}{t}\right)^4 + X_5\left(\frac{a}{t}\right)^5 + X_6\left(\frac{a}{t}\right)^6 \quad (11)$$

for $0 \le a/t \le 0.8$, where t is pipe thickness and the ratio of pipe radius to thickness (R/t) ratio is 20.

For a/t = 0.108, β_T = -0.521 and $K_{J0.2}$ =267MPa√m, as shown in Figure 8.

Based on the above analysis, a value of $K_{J0.2}$=267MPa√m can be derived for the pipeline girth weld, in place of the value $K_{J0.2}$~209MPa√m derived from high-constraint fracture toughness testing, ie the low-constraint value is some 27% higher. Note also that, according to the Annex N approach the value of β_T for an internal flaw in a cylinder (a/t=0.108, β_T=-0.521) is lower (more negative) than that of an SENT specimen (a/W=0.4). This seems to be reasonably consistent with the practice in the offshore pipeline industry, in which SENT specimens with flaw depth 0.2<a/W<0.5 (equivalent to -0.54<β_T<-0.168 using the Annex N equations), are used to model the constraint conditions associated with girth weld flaws.

Comparison of β_T solutions from Annex N with those derived directly from FEA of specimens

The analyses shown above were based on the β_T solutions of Annex N only; in this section, a comparison is made between the Annex N solutions and those derived directly from FEA for the particular specimens tested by Zhou.

The analyses carried out by Zhou are reported in terms of T/σ_Y, where σ_Y is the yield or 0.2% proof strength. In order to express the constraint in terms of β_T, thus allowing a FAD-based analysis, the value $\beta_T = T/(\sigma_Y L_r)$ was calculated, where L_r was calculated from the load corresponding to the value of $J=J_{0.2}$, extracted from the specimen test records. In the case of SENB specimens, which were tested using the unloading compliance technique, this was readily available because load and clip displacement were recorded at regular intervals throughout the test. In the case of SENT specimens, where a multiple specimen method had been used to derive the R-curve, the individual test result closest to $J=J_{0.2}$ was used. This produced a tear length Δa=0.286mm, so the load recorded is an upper bound estimate of the true load at $J=J_{0.2}$.

The values of β_T are compared in Table 2. Results for the SENB specimens were similar regardless of whether Annex N or Zhou's solutions were used. For the case of the SENT specimens, there was a difference between the two solutions, with the more negative values derived from Zhou's work. It may be that the difference between the solutions lies in the respective boundary conditions – the Annex N solution assumes pinned ends, whereas the condition tested (and analysed) by Zhou was that of clamped ends. When the specimen-specific value of β_T is used, ie $\beta_T \le -0.443$ along with

the actual value of $K_{J0.2mm}$ determined by testing, the new datapoint lies very close to the trendline established by SENB testing – see Figure 8 (note, however, that the point may lie to the left of the trend curve, because of the uncertainty in determining the exact value of β_T).

When the hypothetical girth weld is analysed using the low-constraint value of fracture toughness, the analysis point shifts to a lower value of K_r (from 0.498 to 0.412) as shown in Figure 9. This analysis therefore demonstrates the so-called Procedure II of Annex N, ie modification of K_{mat} by matching the constraint of the test specimen to that of the structure. The alternative, but equivalent, is to use Procedure I, in which the FAD is altered to reflect the constraint-dependence of K_{mat}, but high-constraint values of K_{mat} are used in the calculation of K_r.

Residual stress-based assessment (Annex Q)

The basic assessment described earlier assumed the so-called Level 1 residual stress distribution, in which residual stresses act as a uniform membrane stress, the magnitude of which is equal to the yield strength of the parent metal. Annex Q of the new BS 7910 includes a compendium of residual stress distributions for a range of different joint types and welding processes, based on upper-bound fits to experimental data. Figure 10 shows an example of the transverse residual stress distribution (ie the longitudinal stress, relative to the pipe axis) assumed for pipeline girth welds, as a function of through-wall position (x=0 corresponds to the inner surface of the pipe) and welding heat input. It was established that the 'low' heat input curve best described the welding parameters and geometry of the girth weld under consideration. For this situation, the residual stress is assumed to reach yield strength magnitude at both the internal (x=0) and external (x=27.8mm) surfaces, but there is a significant stress gradient over the 0<x<3mm interval corresponding to the extent of the internal circumferential flaw. The effect of applying this stress distribution, via a weight function method, in place of the 'Level 1' residual stress distribution used in the baseline calculations is shown in Figure 11. Other inputs (eg fracture toughness) are as for the basic assessments. As for the constraint-based calculations, a potentially significant reduction in K_r (from 0.498 to 0.390) can be seen when the Annex Q stress distribution is used in place of the Level 1 assumption.

Mismatch assessment (Annex I/P)

The basic analyses assumed the tensile properties to be those of the parent metal, ie the weaker component. It is normal practice in pipeline welding to ensure that the weld metal overmatches the parent material in terms of yield strength, and this can lead to an increase in defect-tolerance relative to the values derived from the basic analyses. As shown in Figure 12, the parent metal considered in the case study showed continuous yielding, and the weld metal discontinuous yielding, with around 20% overmatch at the yield/0.2% proof strength. Whilst the current (2005) edition of BS 7910 generally treats weldments as homogeneous, with properties equal to those of the weaker component, the new BS 7910 allows analysis of mismatched welds via two annexes, P (reference stress/limit load solutions) and I (treatment of mismatch) Annex P of the new BS 7910 contains several 'mismatch-corrected' limit load solutions, including one for a fully circumferential flaw in a pipe. The solution takes into account the ratio of yield strengths (M, where M>1 denotes overmatching) and the size of the weld ('2h' in Figure 2), so that for an overmatching weld of this configuration:

$$\psi = \frac{t-a}{h} \tag{12}$$

$$\frac{F_e^{M(3)}}{F_e^B} = M \quad for\ \psi \le \psi_1 = e^{-2(M-1)/5)} \tag{13}$$

$$\frac{F_e^{M(3)}}{F_e^B} = \frac{24(M-1)}{25}\frac{\psi_1}{\psi} + \frac{M+24}{25} \quad for\ \psi \ge \psi_1 = e^{-2(M-1)/5)}$$

$$\frac{F_e^M}{F_e^B} = \min\left\{\frac{F_e^{M(3)}}{F_e^B}, \frac{1}{1-a/t}\right\} \tag{14}$$

The maximum benefit from mismatch (maximum possible value of F_e^M/F_e^B) is therefore M, but for the particular case considered in the case study, where h is very small, F_e^M/F_e^B=1.03 On this basis, the solution for limit load of a homogeneous material, as given in Annex P of the new BS 7910:

$$F_e{}^B = 2\frac{\sigma_Y{}^B}{\sqrt{3}}\pi\left[r_o{}^2 - (r_i + a)^2\right] \tag{15}$$

A second component of the treatment of mismatched welds is to recalculate the FAL to take account of the mismatch, as described by Annex I of the new procedure. An 'equivalent' material is defined, derived from the properties of the parent and weld metal, and the FAL is the Option 1 FAL, but with variables σ_M, μ_M, N_M in place of σ, μ, N in Equations (1)-(5) and:

$$L_{r,\max} = \frac{1}{2}\left(1 + \frac{0.3}{0.3 - N_M}\right) \tag{16}$$

The effect of this for the girth weld is shown in Figure 13; the 'safe' area has reduced slightly and the value of L_r has fallen slightly, with the result that the overall effect of considering mismatch is negligible. Although in this particular case the 'safe' area has reduced, the general effect of high mismatch and large weld width is to increase the safe area by

enlarging the FAD relative to that FAD for the weaker component.

The analysis shown in Figure 13 is the so-called Option 1M (equivalent to FITNET Option 2), in which M is considered to be a single value, based on the ratio of weld metal to parent metal yield strength. As can be seen from Figure 12, in practice the two stress-strain curves have markedly different shapes, and M is a function of strain. This can be taken into account by using an Option 2M analysis, but in view of the small effect of overmatch when using Option 1M in place of Option 1, Option 2M was not explored as part of this study.

Another aspect of this case is that, if the value F_e^B is calculated as per equation (15), the resulting value of L_r is 0.484 (before correcting for mismatch), considerably lower than the value L_r=0.562 (again, for a homogeneous material) calculated from the current BS 7910 Annex P, a solution derived from the work of Miller [8]. There can thus be two potential solutions to L_r (0.469 or 0.545) after correction for mismatch, depending on which underlying reference stress/limit load solution for homogeneous components is used. For consistency with earlier results, the higher value is assumed in this case. The differences between the limit load solutions for mismatched structures (taken from the FITNET and R6 procedures) and those for homogeneous structures (taken from the current BS 7910) are explored in more detail in another paper at this conference [9].

Summary of case study

The case study has shown that a known flaw analysis can be refined considerably by taking into account crack tip constraint and residual stress distribution in accordance with the clauses of the new BS 7910. For the particular case considered (a narrow-gap girth weld), inclusion of overmatch does not produce any benefit, but in general terms, high levels of overmatch and a large weld width would allow the clauses of Annex N and Annex I to be implemented.

Table 3 summarises the results of the analyses described above, in terms of L_r and K_r. Also shown (Case 6) are the effects of combining residual stress and constraint analysis with the use of an Option 2 FAL. In order to compare all the analyses, the limiting value of membrane stress, $P_{m,crit}$, at which the analysis point lies on the FAL has also been calculated for each case. It can be seen that, although the known flaw analysis showed significant benefits of incorporating constraint and residual stress profile, the safety margin, ie the ratio $P_{m,crit}/P_m$ is not necessarily greatly improved. This is because both the constraint-based analysis and the residual stress analysis of the known flaw are K-dominated, whereas when P_m is incremented until the FAL is reached, the analysis becomes collapse-dominated.

REFERENCES

[1] BS 7910:2005 (incorporating Amendment 1, published in 2007); 'Guide to Methods for Assessing the Acceptability of Flaws in Metallic Structures', BSI, 2005.

[2] R6: Assessment of the Integrity of Structures containing Defects, Revision 4, 2001, including updates to Amendment 8, 2010, British Energy Generation Ltd, Gloucester.

[3] FITNET Fitness-for-Service (FFS) - Procedure (Volume 1) ISBN 978-3-940923-00-4 (Koçak, M, Webster, S, Janosch, JJ, Ainsworth, RA and Koers, R) and FITNET Fitness-for-Service (FFS) - Annex (Volume 2) ISBN 978-3-940923-01-1, (Koçak, M, Hadley, I, Szavai, S, Tkach, Y and Taylor, N) both printed by GKSS Research Center, Geesthacht, 2008.

[4] Hadley, I: PVP 2009-78057: BS 7910: 'History and Future Developments'.

[5] Hadley, I, Ainsworth, R, Budden, P and Sharples, J: PVP 2010-25582: 'The Future of the BS7910 Flaw Assessment Procedure'.

[6] Zhou, DW: 'J-R curve testing using single edge-notched tensile (SENT) specimens', European Conference on Fracture (ECF18), 2010; August 30 to September 03 2010, Dresden, Germany.

[7] Zhou, DW: 'Measurement and modelling of R-curves for low-constraint specimens', Engineering Fracture Mechanics 78 (2011) 605–622.

[8] Miller, AG: 'Review of limit loads of structures containing defects', CEGB report TPRD/B/0093/N82 Rev.1, Berkeley, Gloucester, UK, 1984.

[9] Eren, E, Hadley, I and Nikbin, K: PVP2011-57255, 'Differences in the Assessment of Plastic Collapse in BS 7910:2005 and R6/FITNET FFS Procedures'.

Grade	X65 (SMYS=448N/mm^2, SMTS=530N/mm^2
OD	970mm (nominal 38")
WT	27.8mm (1.09")
Tensile properties of parent (base) material	0.2% proof strength: 478N/mm^2 UTS: 583N/mm^2
Yield behaviour of parent material	Continuous
Tensile properties of weld metal	0.2% proof strength: 575N/mm^2 UTS: 653N/mm^2
Yield behaviour of weld metal	Discontinuous
Width of weld at pipe mid-thickness (2h)	6.5mm
Flaw size and position	3mm high fully circumferential internal (root) flaw at weld centreline
Fracture toughness of weld metal	Determined at room temperature using tearing resistance curves (R-curves), from both high- and low-constraint specimens
Weld condition	As-welded
Applied stress	Axial stress of 239N/mm^2, ie 50% of the actual parent metal yield strength

Table 1: Characteristics of pipeline considered in the case study

Specimen	β_T, Annex N	T/σ_Y, from FEA	$\beta_T = T/(\sigma_0 L_r)$
SENB, a/W=0.16	-0.427	-0.41	-0.416
SENB, a/W=0.35	-0.065	0.019	-0.062
SENB, a/W=0.51	0.092	0.125	0.094
SENB, a/W=0.70	0.180	0.084	0.187
SENT, a/W=0.4	-0.328	-0.326	≤-0.443

Table 2: Comparison of Annex N constraint parameters with those derived by Zhou
Note: the L_r solutions of Annex N were used

No.	K_{mat}, MPa√m	RS	Tensile properties	FAD	L_r	K_r	$P_{m,crit}$, N/mm^2
0	209	Level 1	PM, σ_Y and σ_{UTS} only	BS Level 2a	0.562	0.498	442
1	209	Level 1	PM, σ_Y and σ_{UTS} only	Opt 1	0.562	0.498	432
2	209	Annex Q	PM, σ_Y and σ_{UTS} only	Opt 1	0.562	0.390	440
3	267	Level 1	PM, σ_Y and σ_{UTS} only	Opt 1	0.562	0.412	443
4	209	Level 1	'equivalent' tensile properties	Opt 1M	0.545	0.498	443
5	209	Level 1	PM, actual stress-strain curve	Opt 2	0.562	0.498	451
6	267	Annex Q	PM, actual stress-strain curve	Opt 2	0.562	0.322	467

Table 3: Summary of analyses

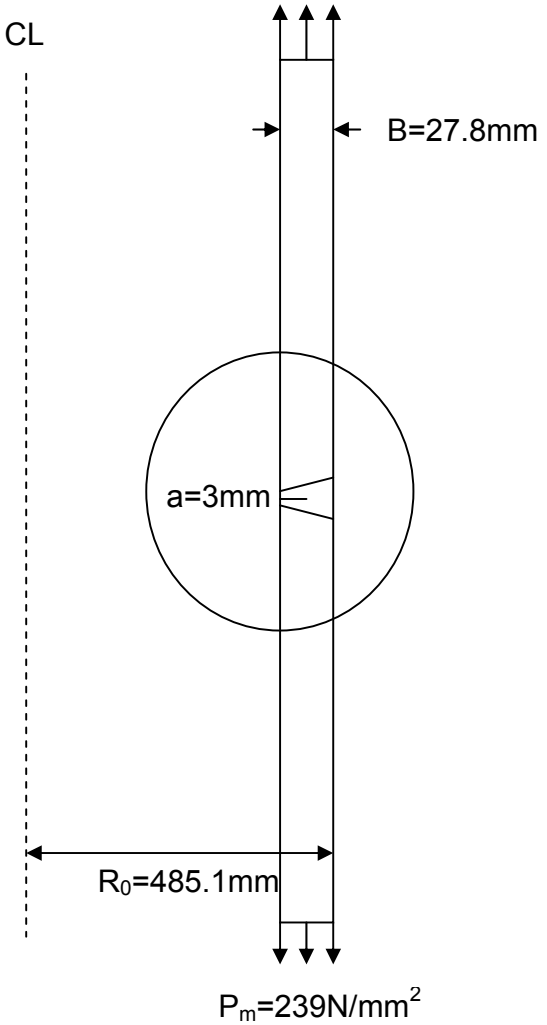

Figure 1 Geometry of pipeline girth weld

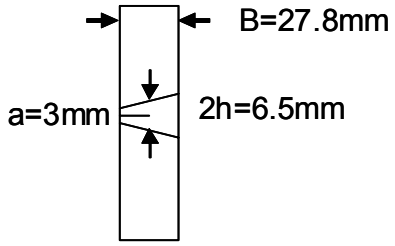

Figure 2 Detail of weld area (circled in Figure 1)

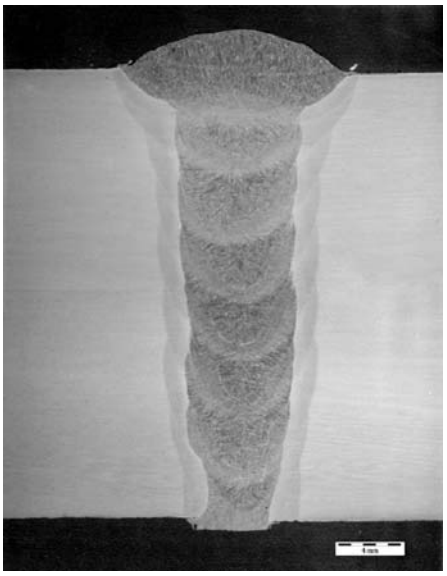

Figure 3 Macro of weld considered

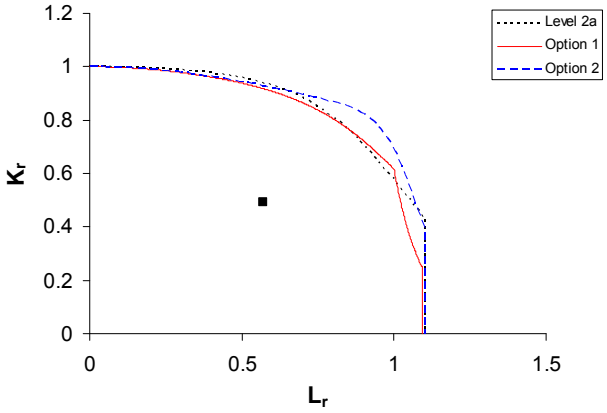

Figure 4 Results of analysis using Options 1 and 2, and comparison with the current BS 7910:2005 Level 2a method

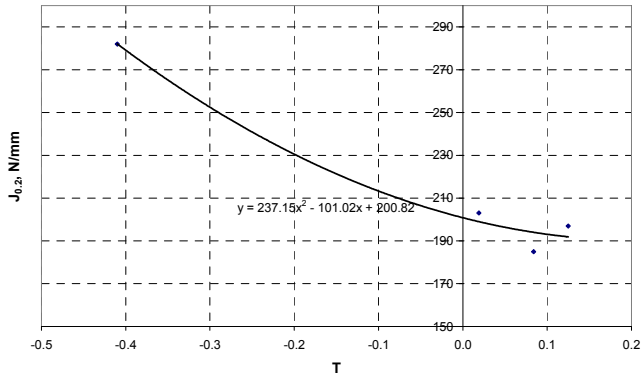

Figure 5 Relationship between elastic T-stress and initiation toughness ($J_{0.2mm}$) for SENB specimens

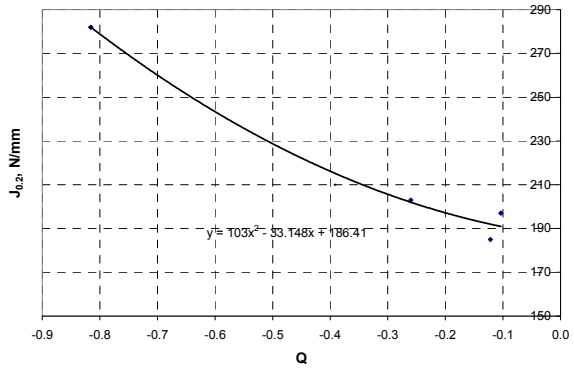

Figure 6 Relationship between Q and initiation toughness ($J_{0.2mm}$) for SENB specimens

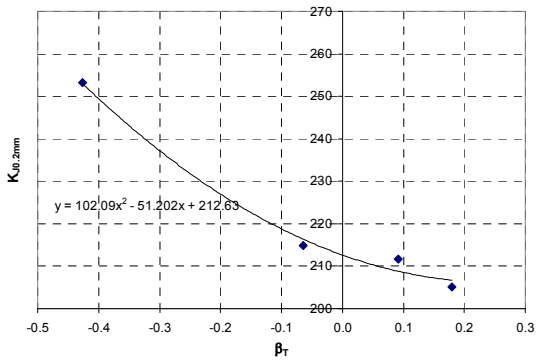

Figure 7 Relationship between β_T and initiation toughness ($K_{J0.2mm}$) for SENB specimens

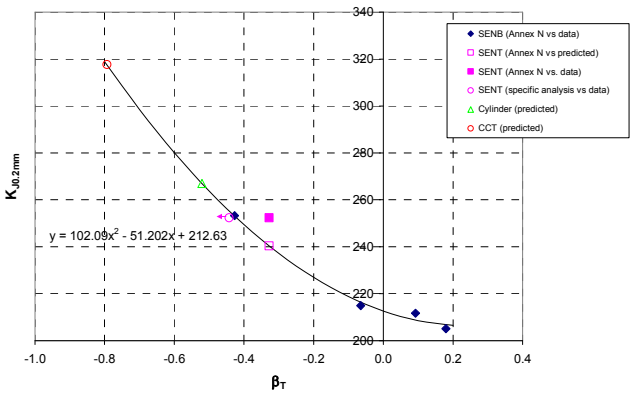

Figure 8 Summary of results for SENB and SENT specimens, and predicted values of $K_{J0.2mm}$ for CCT specimens and a circumferentially cracked pipe

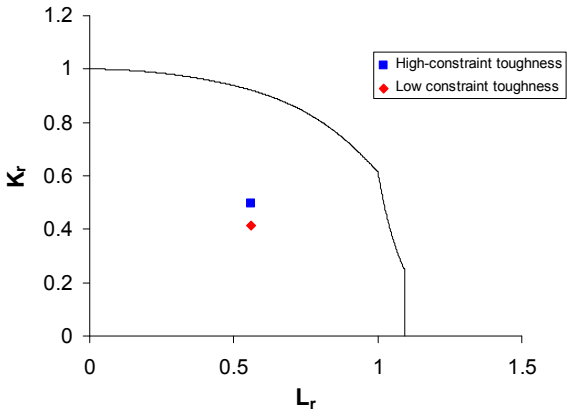

Figure 9 FAD showing results based on high- and low-constraint specimens

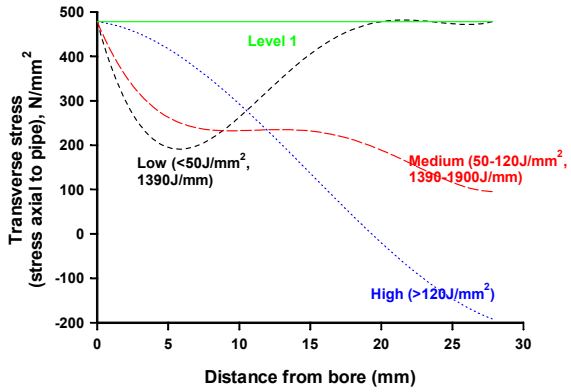

Figure 10 Residual stress distributions for girth welds, from Annex Q of the new BS 7910. The stresses shown are perpendicular to the weld, ie along the pipe axis

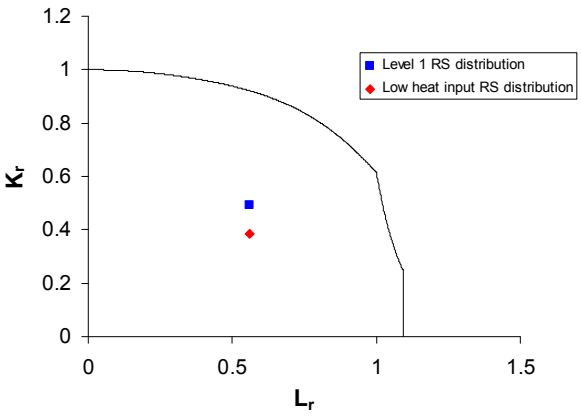

Figure 11 Results of FAD-based analysis, comparing Level 1 residual stress assumption with the use of Annex Q

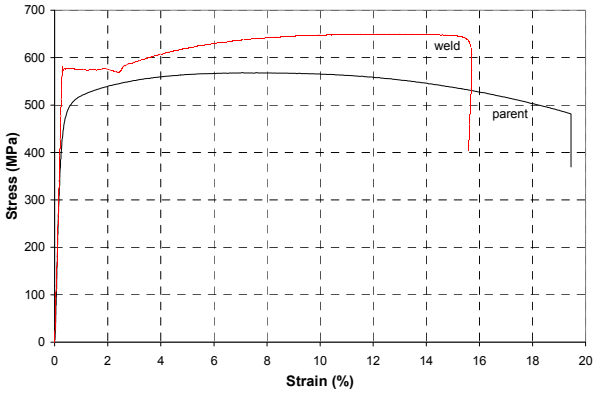

Figure 12 Stress-strain curves for parent and weld metal

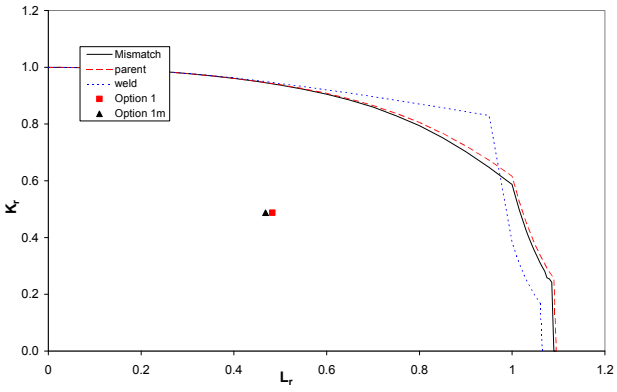

Figure 13 FAD-based analysis of mismatched weld; M=1.2 and 2h=6.5mm